Table V. L-L-V Locus End Points for the Four Binary Systems Studied and Also for the Binary Systems CO_2-*n*-Decane (*4*) and CO_2-*n*-Eicosane (3)

system	type	temp, K	press., bar	CO_2 mole fraction L_1	CO_2 mole fraction L_2	molar vol, mL/(g-mol) v_{L_1}	molar vol, mL/(g-mol) v_{L_2}
CO_2-C_{12}	Q	235.66	10.58	0.577	0.974	103.2	44.1
CO_2-C_{10}	UCST	248.75	16.37	0.850	0.850	63.9	63.9
CO_2-C_{12}	Q	254.28	20.06	0.657	0.9749	104.7	47.5
CO_2-C_{12}	UCST	267.37	28.82	0.870	0.870	68.3	68.3
CO_2-C_{13}	Q	255.16	20.76	0.611	0.9842	117.2	46.2
CO_2-C_{13}	UCST	278.95	39.33	0.860	0.860	74.4	74.4
CO_2-C_{14}	Q	269.10	30.82	0.703	0.9821	105.9	50.6
CO_2-C_{14}	K	311.15	82.60	0.840		77.3	
CO_2-C_{15}	Q	270.40	31.94	0.680	0.9883	117.8	49.3
CO_2-C_{15}	K	309.41	80.22	0.788		98.1	
CO_2-C_{20}	Q	300.41	67.48	0.723	0.998	139.5	63.5
CO_2-C_{20}	K	305.31	75.49	0.704		131.6	

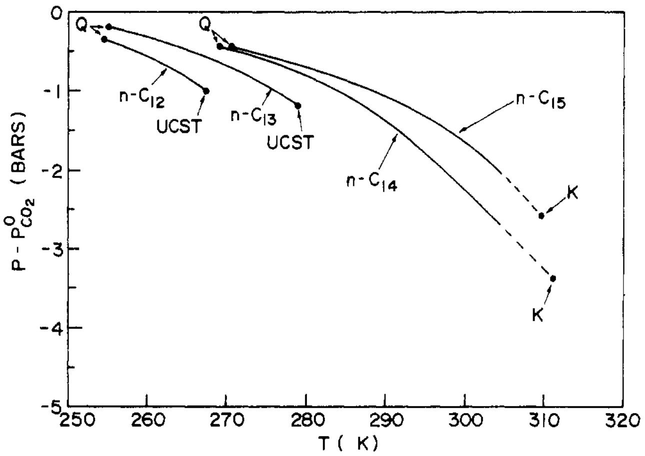

Figure 3. Deviation (smoothed) of the *P* vs. *T* curves of the L-L-V loci from the vapor-pressure curve of pure CO_2. $P^0_{CO_2}$ is the vapor pressure of pure CO_2. For temperatures exceeding the critical temperature of pure CO_2, the following equation for (hypothetical) $P^0_{CO_2}$ was employed: $P^0_{CO_2} = \exp(15.4437 - 1990.0/T) + 0.21136(T - 288.15)^2 - 18.47$, where $P^0_{CO_2}$ is in bar and *T* is in K.

decane (*2*) and CO_2-*n*-eicosane (*3*) systems. Note that the L_1-L_2-V locus decreases in extent in *P*-*T* space with increasing carbon number for those systems having a K point. For those systems having a UCST, the locus moves in *P*-*T* space to higher values of both variables and exhibits a lengthening, with increase of carbon number at least with respect to *n*-dodecane and *n*-tridecane.

All of the L_1-L_2-V loci studied exhibit an L_2 phase very rich in CO_2. Since the vapor phase is virtually pure CO_2, the L_1-L_2-V loci are close in *P*-*T* space to the L-V locus of pure CO_2. Figure 3 illustrates this proximity by showing $P-P^0_{CO_2}$ (smoothed) vs. *T* for each binary L_1-L_2-V system, where $P^0_{CO_2}$ is the vapor pressure of pure CO_2. The deviation of *P* from $P^0_{CO_2}$ is small and negative in all cases examined.

Glossary

K	K point, where L_2 and V phases become critical in the presence of L_1 phase
L	Liquid phase
L_1	liquid 1 phase
L_2	liquid 2 phase
P	pressure
T	temperature
UCST	upper critical solution (temperature) point where L_1 and L_2 phases become critical in presence of V phase
v	molar volume
V	vapor phase
x_i	mole fraction of species *i*

Literature Cited

(1) Fussell, L. T. "A Technique for Calculating Phase Equilibria of Three Coexisting Hydrocarbon Phases", SPE paper 6722, presented at the 52nd Annual Fall Technical Conference and Exhibition of the SPE of AIME, Denver, CO, Oct 9-12, 1977.
(2) Schneider, G. *Chem. Eng. Prog., Symp. Ser.* **1968**, *64*, 9-15.
(3) Kulkarni, A. A.; Zarah, B. Y.; Luks, K. D.; Kohn, J. P. *J. Chem. Eng. Data* **1974**, *19*, 92-4.
(4) Huie, N. C.; Luks, K. D.; Kohn, J. P. *J. Chem. Eng. Data* **1973**, *18*, 311-3.
(5) McCaffrey, D. S.; Kohn, J. P. *Chem. Eng. Prog., Symp. Ser.* **1968**, *64*, 22-33.
(6) Rossini, F. D.; Pitzer, K. S.; Arnett, R. L.; Braun, R. M.; Pimentel, G. C. "Selected Values of Physical and Thermodynamic Properties of Hydrocarbons and Related Compounds", API Research Project 44; Carnegie Press: Pittsburgh, PA, 1953.
(7) Din, F. "Thermodynamic Function of Gases"; Butterworths: London, 1956; pp 102-34.

Received for review April 4, 1980. Accepted March 19, 1981. The apparatus used was constructed under grants from the National Science Foundation.

Activities of Gallium-Thallium Components Determined by Vapor-Pressure Data

Raffaele Mastromarino, Vincenzo Piacente,* and Daniela Ferro

Istituto di Chimica Fisica, Università degli Studi, 00185 Roma, Italy

The thallium activity in liquid Ga-Tl alloys was determined at 1000 K from vapor-pressure data. Mixing thermodynamic parameters of both components were evaluated and compared with those reported in the literature. A quadratic formalism for the activity coefficients and the enthalpic functions of the alloy components were derived.

Introduction

In order to complete the systematic investigation of the binary systems having as constituents Ga, Zn, and Tl (*1*, *2*) for taking these results into consideration for a future ternary system study and in connection with the use of thallium alloys as molecular sources of Tl in thermodynamic equilibria involving this constituent (*3*), we have determined the activities of the

0021-9568/81/1726-0258$01.25/0

Table I. Summary of the Torsion Effusion Measurements

run	Tl composition, at. %	temp range, K	no. of points	$\log \alpha = A - B/T$[a] A	B	activity at 1000 K
78.03	8.0	952-1010	12	10.13 ± 0.21	8259 ± 296	0.460
78.09	12.1	879-989	13	10.29 ± 0.28	8346 ± 302	0.546
78.10	5.4	875-953	11	9.90 ± 0.34	8140 ± 214	0.357
78.12	10.5	883-1035	15	10.44 ± 0.22	8492 ± 219	0.551
b	100	826-1077	46	11.12 ± 0.23	8913 ± 213	1.000

[a] The quoted errors are standard deviations. [b] Average of four vaporization runs.

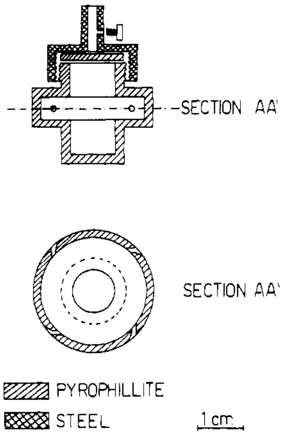

Figure 1. Schematic diagram of the torsion effusion cell.

elements in liquid Ga-Tl alloys. Apparently the only activity values available are those derived by Predel (4, 5) from calorimetric data and those measured by Danilin (6) by the emf technique. Mixing enthalpies of this system were calculated by Sommer (7) using a model potential. No direct activity measurements are reported in the literature. Therefore, we thought it useful to fill this gap by carrying out direct measurements of thallium activity measuring its vapor pressure with a multiple rotating Knudsen cell coupled with a mass spectrometer and a torsion effusion apparatus.

Experimental Section

Some Ga-Tl alloys of low thallium content and two alloys of 52 and 83 at.% Tl were prepared by using spectrographically pure elements. Appropriate weights of the two metals were introduced in a tantalum liner, evacuated, sealed, and melted by heating up to 1100 K for several hours inside a steel cell. The melted alloys were quenched, and their homogeneity and composition were checked by chemical and polarographic analyses. In some cases this check was also made at the end of the vaporization experiment in order to test the absence of significant depauperization of the most volatile component. The results of these analyses agreed with the original compositions within ~0.1-0.3 at. % Tl. The vaporization of the alloys was studied by using a mass spectrometer and a torsion effusion apparatus, and the thallium vapor pressure was measured.

Torsion Effusion. The thallium activities for alloys of low thallium content were determined by the torsion effusion technique. The basis of the method and the experimental apparatus have been described in detail elsewhere (8, 9). The effusion cell, illustrated in Figure 1, was derived from a block of pyrophyllite. At each temperature the sample vapor pressure can be determined by measuring the cell deflection (α) through the well-known relation (8) $P = \alpha K$, where K takes into account the cell constants (10), the torsion constant of the tungsten torsion filament, and, of course, the pressure unit.

Using the same cell for pure thallium and for its alloys, we directly derived the activity of this element from the ratio of the torsion angles measured at the same temperature. Most of the systematic errors associated with the absolute K value are eliminated by doing so. Alloys with the compositions 5.4, 8.0, 10.5, and 12.1 at. % Tl were investigated. In Table I are reported the slopes and the intercepts of the torsion angle-temperature equations in the covered temperature range as obtained by the least-squares treatment of the experimental results. Because of the low thallium content of the analyzed alloys, only the initial points measured in the first step of the vaporization were taken into consideration. Some checks of the sample composition at the end of the experiments were made. For the activity calculation the average equation $\log \alpha^0 = (11.12 \pm 0.12) - (8913 \pm 213)/T$ for pure thallium was used. In order to test that thermodynamic equilibrium conditions exist in the used cell, absolute vapor pressures of some pure elements (zinc, lead, and thallium) were measured, and their corresponding heats of vaporization, determined by second- and third-law treatment of the vapor-pressure data, were compared with those selected by Hultgren et al. (11). The results are in very good agreement within the associated errors.

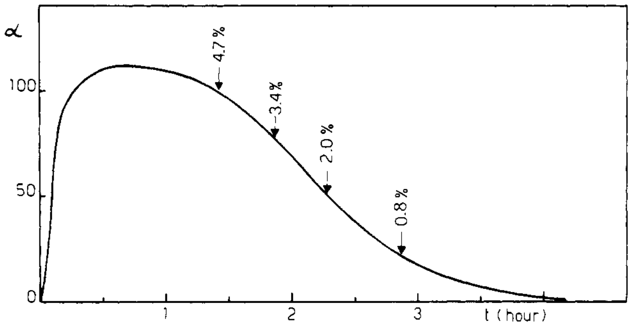

Figure 2. Plot of torsion angles vs. time measured during the quantitative vaporization of Tl at the fixed temperature of 1027 K.

With this technique the thallium activity was also measured by the quantitative vaporization of this element from the alloys following a procedure similar to that described in a previous work (12). These experiments were carried out by loading a known amount of alloy and by vaporizing completely the thallium at a constant temperature. The deflection angles were measured as a function of the vaporization time while the thallium content in the alloy was decreasing. According to the Knudsen equation (13) the area of the α-time plot is proportional to the weight loss of the sample. Therefore, after complete vaporization of the thallium from a sample of known weight and composition, deflection angles corresponding to the preselected compositions 4.8, 3.4, 2.0, and 0.8 at. % Tl were determined on the plot. A panoramic view of vaporization behavior (run 78.15) is graphically reported as α vs. time in Figure 2. The log α values obtained from seven quantitative vaporizations are reported in Table II and plotted as a function of the temperature in Figure 3. Although it is difficult to determine accurately the errors associated with these data, their evaluation leads to a very small uncertainty in the composition (~0.2%) and a larger one in the torsion angle (~5%). By the least-squares treatment of the data, the log α-temperature equations corresponding to each composition were derived and reported in Table II.

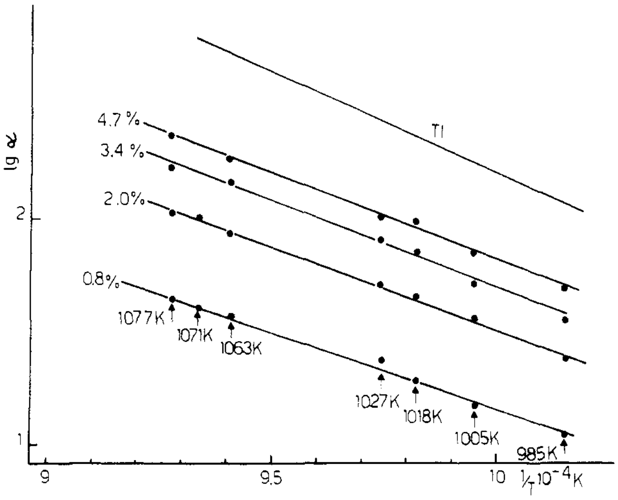

Figure 3. Plot of log vs. 1/*T* for 4.7, 3.4, 2.0, and 0.8 at. % Tl during the quantitative vaporizations.

Table II. Quantitative Vaporization Results

run	original Tl composition, at. %	T, K	log α 4.7 at. % Tl	3.4 at. % Tl	2.0 at. % Tl	0.8 at. % Tl
78.04	5.7	1071			2.00	1.60
78.05	9.6	1077	2.36	2.22	2.02	1.64
78.08	7.4	985	1.69	1.55	1.38	1.05
78.13	5.0	1005	1.85	1.71	1.56	1.17
78.15	9.9	1027	2.00	1.90	1.70	1.36
78.16	8.6	1018	1.98	1.85	1.65	1.28
78.19	10.7	1063	2.26	2.15	1.93	1.56

log α vs. 1/*T* equations:

alloy, 4.7 at. % Tl	$\log \alpha = (9.46 \pm 0.15) - (7647 \pm 152)/T$
alloy, 3.4 at. % Tl	$\log \alpha = (9.48 \pm 0.19) - (7796 \pm 195)/T$
alloy, 2.0 at. % Tl	$\log \alpha = (8.81 \pm 0.11) - (7301 \pm 116)/T$
alloy, 0.8 at. % Tl	$\log \alpha = (7.97 \pm 0.25) - (6814 \pm 255)/T$

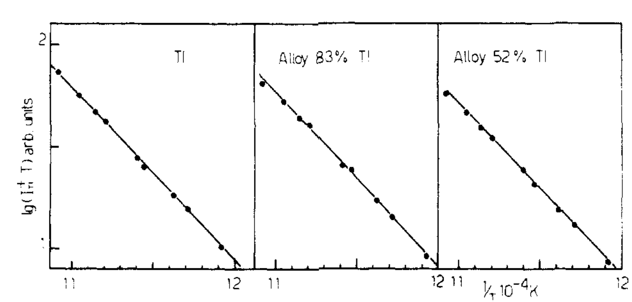

Figure 4. Ion intensity dependence from temperature, determined by mass-spectrometric technique.

Mass Spectrometry. The thallium activities in high-thallium alloys were measured by using a Bendix time of flight mass spectrometer (Model 3015) coupled with a pyrophyllite multiple rotating Knudsen cell with three housings. The details of the method and of the experimental procedure are reported in a previous work (*14*). Two alloys, 52 and 83 at. % Tl, were studied by this technique in the temperature range 838–915 K. At each experimental temperature some series of Tl^+ ion intensity values were measured by rotating the cell, and their average values are reported in Table III and plotted in Figure 4 as log ($I_{Tl}{}^+T$) vs. 1/*T*. The intensity values have been corrected by calibration factors which account for possible differences in the geometry of the effusion holes and their nonperfect alignment during the rotation of the cell. The factors (x_i) were determined by loading the three crucibles with pure thallium and by recording the Tl^+ ion intensity corresponding to each crucible. With crucible 1 ($x_1 = 1.00$) as a standard, the average values $x_2 = 1.07 \pm 0.01$ and $x_3 = 0.925 \pm 0.01$, for crucibles 2 and 3, respectively, were determined. From the least-squares treatment of the mass-spectrometric data, the following equations were derived:

$$\text{Tl, pure} \quad \log (I^+T) = (6.73 \pm 0.05) - (8891 \pm 87)/T$$

$$\text{alloy, 83 at. \% Tl} \quad \log (I^+T) = (6.74 \pm 0.11) - (8628 \pm 96)/T$$

$$\text{alloy, 52 at. \% Tl} \quad \log (I^+T) = (6.62 \pm 0.13) - (8860 \pm 115)/T$$

Results and Discussion

The thallium activity in the analyzed liquid Tl-Ga alloys was determined at 1000 K from the torsion data by using the relation

$$a_{Tl} = \exp(A_i - B_i/T) \exp[-(A^0 - B^0/T)]$$

in which A^0, A_i, B^0, and B_i are the intercepts and the slopes of log α – 1/*T* equations for pure thallium and thallium in alloy reported in Table I. The activity values so obtained are plotted in Figure 4 as a function of N_{Tl}. In the same figure are also reported the thallium activities of 0.8, 2.0, 3.4, and 4.8 at. % Tl obtained from the quantitative vaporization experiments using the values derived at 1000 K from the equations reported in Table II. The value $\alpha^0 = 161$ for pure thallium was used. The activities 0.94 and 0.83 in the liquid alloys of 85 and 53 at. % Tl, respectively, were derived from the mass-spectrometric data reported previously at the average temperature $T = 880$ K. These values were derived from the ion intensity ratios $a = I^+(\text{alloy})/I^+(\text{pure})$ taking into account the correlation of the vapor pressure *P* with the measured ion intensities: $P = I^+TK$ (*15*) (*K* is an instrument constant for a given species). The activity values so determined are reported in Figure 5. In the same figure Predel's (*5*) and Danilin's (*6*) data are also reported. Our data agree very well with Danilin's activities for the alloy ranging in the high-gallium compositions while they show a larger positive deviation in the thallium-rich alloys. This dis-

Table III. Tl^+ Ion Intensities[a] Measured by Mass-Spectrometric Technique over Ga–Tl Alloys

T, K	no. of points	Tl pure (crucible 1)	83 at. % Tl alloy (crucible 2)	52 at. % Tl alloy (crucible 3)
838 ± 2[b]	2	$(19.0 \pm 0.5) \times 10^{-8}$ [b]	$(17.0 \pm 0.5) \times 10^{-8}$ [b]	$(15.5 \pm 0.5) \times 10^{-8}$ [b]
858 ± 2	4	$(28.0 \pm 0.5) \times 10^{-8}$	$(26.0 \pm 0.5) \times 10^{-8}$	$(24.0 \pm 0.5) \times 10^{-8}$
862 ± 3	2	$(33.5 \pm 0.5) \times 10^{-8}$	$(31.5 \pm 0.5) \times 10^{-8}$	$(26.0 \pm 0.5) \times 10^{-8}$
873 ± 3	1	$(45.0 \pm 1.0) \times 10^{-8}$	$(43.0 \pm 1.0) \times 10^{-8}$	$(37.0 \pm 1.0) \times 10^{-8}$
876 ± 2	4	$(50.0 \pm 0.5) \times 10^{-8}$	$(46.0 \pm 0.5) \times 10^{-8}$	$(43.0 \pm 0.5) \times 10^{-8}$
892 ± 3	3	$(74.0 \pm 1.0) \times 10^{-8}$	$(71.0 \pm 0.5) \times 10^{-8}$	$(61.0 \pm 1.0) \times 10^{-8}$
896 ± 2	3	$(82.0 \pm 2.0) \times 10^{-8}$	$(77.0 \pm 1.0) \times 10^{-8}$	$(70.0 \pm 2.0) \times 10^{-8}$
903 ± ?	1	$(98.0 \pm 2.0) \times 10^{-8}$	$(91.0 \pm 2.0) \times 10^{-8}$	$(80.0 \pm 2.0) \times 10^{-8}$
915 ± 2	3	$(12.5 \pm 0.5) \times 10^{-7}$	$(11.0 \pm 0.5) \times 10^{-7}$	$(9.7_5 \pm 0.5) \times 10^{-7}$

[a] Arbitrary units. The values are corrected for the factor of the used rotating cell (see text). [b] The associated error is the semidispersion in the experimental measurements.

Table IV. Thermodynamic Properties at 1000 K

N_{Tl}	a_{Tl}	a_{Ga}	$-\Delta\overline{G}_{Tl}{}^{mix}$, kcal/mol	$-\Delta\overline{G}_{Ga}{}^{mix}$, kcal/mol	$\Delta\overline{G}_{Tl}{}^{ex}$, kcal/mol	$\Delta\overline{G}_{Ga}{}^{ex}$, kcal/mol	$-\Delta G^{mix}$, kcal/mol	ΔH^{mix},[a] kcal/mol	ΔS^{mix}, cal/mol K
0.1	0.52	0.94	1.300	0.123	3.276	0.086	0.240	0.375	0.615
0.2	0.64	0.90_5	0.887	0.198	2.311	0.245	0.336	0.665	1.001
0.3	0.71	0.87_5	0.680	0.265	1.712	0.443	0.389	0.763	1.152
0.4	0.76	0.84_5	0.545	0.335	1.276	0.680	0.419	0.880	1.299
0.5	0.81	0.80	0.419	0.443	0.959	0.934	0.431	0.880	1.311
0.6	0.86	0.75	0.300	0.572	0.715	1.249	0.409	0.875	1.284
0.7	0.90	0.69	0.209	0.737	0.500	1.655	0.367	0.835	1.202
0.8	0.94	0.61	0.123	0.982	0.320	2.216	0.295	0.673	0.968
0.9	0.98	0.50_5	0.040	1.358	0.169	3.218	0.172	0.400	0.572

[a] Taken from ref *5* at 923 K.

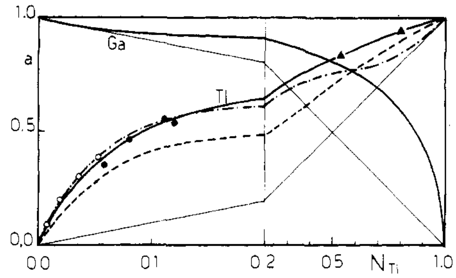

Figure 5. Thallium and gallium activities in liquid alloys: (●) torsion effusion data (1000 K); (O) quantitative vaporization (1000 K); (n▲) mass-spectrometric data (880 K); (- - -) Predel's data (*5*) (923 K); (-·-) Danilin's data (*6*).

agreement cannot be attributed to the temperature difference since the slopes for the alloys at high thallium content are quite similar to those for pure thallium. In any case, in the entire concentration range thallium exhibits a large positive deviation from Rault's law, and this nonideal behavior is to be expected, since the system shows a wide miscibility gap at lower temperature (*4*).

The gallium activity has been derived in the usual way by a graphical integration of the Gibbs-Duhem equation (*16*). The values $\beta = \ln \gamma_{Tl}/(1 - N_{Tl})^2$ necessary for this integration were evaluated for the investigated alloys by using the relation

$$\beta = [(A_x - A^0) - (B_x - B^0)/T - \ln N_{Tl}](1 - N_{Tl})^{-2}$$

The activities of both components and the corresponding partial and integral molar free energy values at 0.1 molar fraction intervals across the system at 1000 K are summarized in Table IV and in Figure 6.

In order to complete the thermodynamic properties of the Ga-Tl alloy, using the $\Delta\overline{H}_{mix}$ reported in the literature (*4*), $\Delta\overline{S}_{mix}$ was derived and reported in the same table. Considering the errors associated with the slopes of our pressure-temperature equations and the fact that most of the studied alloys are grouped in the terminal gallium-rich region, we have preferred to use the $\Delta\overline{H}_{Tl}$ measured by Predel at lower temperature (923 K) for $\Delta\overline{H}_{mix}$ calculations in the entire concentration range.

Darken showed (*17*, *18*) that many metallic solutions exhibit a quadratic formalism for the activity coefficients of component 1 (solvent) and component 2 (solute) which is given by

$$\log \gamma_1 = x_{12}(1 - N_1)^2$$

$$\log \gamma_2 = x_{12}(1 - N_2)^2 + A$$

where x_{12} and A are constants that must be calculated empirically. These constants were derived in Figure 7 by plotting $\log \gamma_{Tl}$ against $(1 - N_{Tl})^2$. The plot is well represented by a

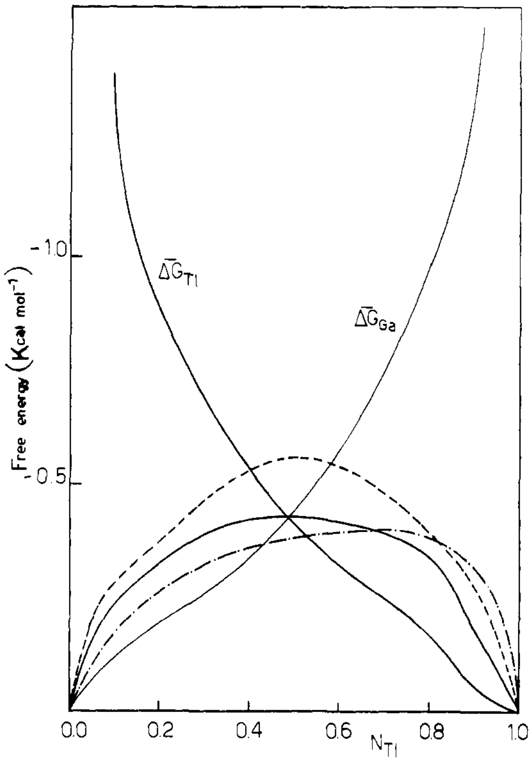

Figure 6. Partial and integral molar free energies of Ga-Tl alloys.

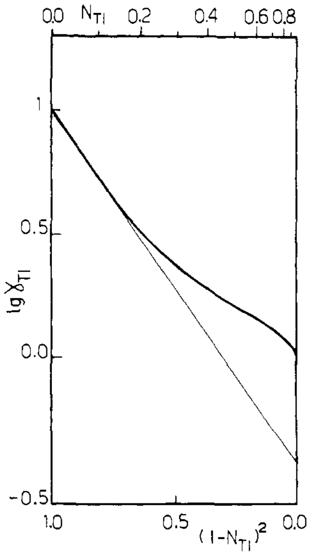

Figure 7. Plot of $\log \gamma_{Tl}$ vs. $(1 - N_{Tl})^2$.

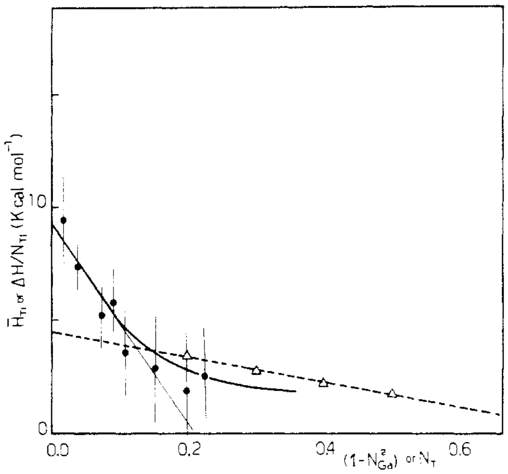

Figure 8. Thallium heat of solution in Ga–Tl alloys.

straight line in the region $0 < N_{Tl} < 0.2$, and the least-squares treatment of the data yields the following equation:

$$\log \gamma_{Tl} = 1.43(1 - N_{Tl})^2 - 0.42$$

so that

$$\log \gamma_{Ga} = 1.43(1 - N_{Ga})^2$$

The χ_{Tl-Ga} value was not calculated for the opposite region, because of the uncertainties in the data. As discussed by Turkdogan and Darken (*19*), if the quadratic formalism is extended to enthalpic functions, the following equation

$$\overline{\Delta H}_2 = \overline{\Delta H}^0{}_2 - B(1 - N_1^2)$$

can be applied, where $\overline{\Delta H}^0{}_2$ is the solute enthalpy of mixing at infinite dilution and B is a characteristic parameter of the studied system. From this equation the following expression for the molar heat of mixing, ΔH, was derived:

$$\Delta H/N_2 = \overline{\Delta H}^0{}_2 - BN_2$$

Our $\overline{\Delta H}_{Tl}$ values, obtained as differences between the vaporization enthalpy of pure Tl at 1000 K selected by Hultgren (*11*) and those derived from the pressure–temperature slopes for each studied alloy at the same temperature, were plotted against $1 - N_{Ga}^2$ in Figure 8 with their experimental uncertainties. An analysis of the data shows a limit of linearity up to 0.1 at. % Tl and gives the equation

$$\Delta H_{Tl} = (9 \pm 1) - (42 \pm 5)(1 - N_{Ga}^2)$$

where the associated errors are estimated. In the same figure the $\Delta H/N_{Tl}$, obtained from Predel's calorimetric data against N_{Tl}, are also reported. Owing to the fact that our measurements are effected by large uncertainties, we feel that $\Delta H^0{}_{Tl}$ = 4.5 kcal/mol derived from Predel's data (*4*) can be taken as a lower limit. Therefore we propose 8 ± 2 kcal/mol as the most probable value of the thallium enthalpy of mixing at infinite dilution.

Acknowledgment

Thanks are due to Professor G. Bruzzone for his kind collaboration in the alloy preparations.

Literature Cited

(1) Piacente, V.; Desideri, A.; Hallgass, A. *Rev. Int. Hautes Temp. Refract.* **1973**, *10*, 85.
(2) Ferro, D.; Piacente, V.; Nappi, B. M. *J. Chem. Eng. Data* **1980**, *25*, 3.
(3) See: Picente, V.; Malaspina, L. *J. Chem. Phys.* **1972**, *56*, 1780, 1978.
(4) Predel, B. *Z. Metallkunde* **1959**, *50*, 663.
(5) Predel, B.; Stein, D. W. *J. Less-Common Met.* **1971**, *24*, 159.
(6) Danilin, V. N.; Jatsenko, S. P. *Zh. Fiz. Khim.* **1967**, *41*, 879.
(7) Sommer, F. *Z. Metallkunde* **1974**, *65*, 788.
(8) Freeman, R. D. In "The Characterization of High Temperature Vapors"; Margrave, J. L., Ed.; Wiley: New York, 1967.
(9) Piacente, V.; DeMaria, G. *Ric. Sci.* **1969**, *39*, 549.
(10) Freeman, R. D.; Searcy, A. W. *J. Chem. Phys.* **1954**, *22*, 762.
(11) Hultgren, R.; Orr, R. L.; Kelley, K. K. "Supplement to Selected Values of Thermodynamic Properties of Metals and Alloys"; Department of Mineral Technology, University of California, 1967.
(12) Ferro, D.; Nappi, B. M.; Piacente, V.; Cignini, P. L. *High Temp. Sci.* **1978**, *10*, 131.
(13) Knudsen, M. *Ann. Phys.* (*Leipzig*) **1909**, *28*, 333.
(14) De Maria, G.; Piacente, V. *Bull. Soc. Chim. Belg.* **1972**, *81*, 155.
(15) Inghram, M. G.; Drowart, J. In "High Temperature Technology"; McGraw-Hill, London, 1960.
(16) Wagner, C. In "Thermodynamics of Alloys"; Addison-Wesley: London, 1952; p 16.
(17) Darken, L. S. *Trans. AIMe* **1967**, *238*, 60.
(18) Turkdogan, E. T.; Darken, L. S. *Trans. AIME* **1968**, *242*, 1997.

Received for review June 9, 1980. Accepted January 21, 1981.